Damage Assessment of a Sixteen Story Building Following the 2017 Central Mexico Earthquake

Yijun Liao[1], Richard L. Wood[2], M. Ebrahim Mohammadi[3], Kanchan Devkota[4], Christine E. Wittich[5]

[1] Ph.D. Student, Department of Civil Engineering, University of University - Lincoln, NE, USA.
[2] Assistant Professor, Department of Civil Engineering, University of University - Lincoln, NE, USA. [3] Ph.D. Candidate, University of University - Lincoln, NE, USA. [4] Graduate Student Researcher, University of University - Lincoln, NE, USA.
[5] Assistant Professor, Department of Civil Engineering, University of University - Lincoln, NE, USA.

ABSTRACT

The 2017 M7.1 Central Mexico Earthquake caused significant infrastructural damage in the Mexico City area. The earthquake contained a significant pulse in the long period, resulting in numerous buildings severely damaged or collapsed. This paper discusses a reinforced concrete building which was still partially occupied post-earthquake. The building's interior walls were examined to have substantial damage, including some extensive cracking. In January 2018, the authors visited the structure and collected detailed assessment data. The data collection included ground-based lidar scans and recorded ambient vibrations of the damaged structure using accelerometers. Eleven scans were collected from the four exterior facades to create a three-dimensional point cloud of the building. The collected point cloud data were used to measure and quantify the permanent deformation of the structure at three corners as well as to generate depth maps of two parallel exterior walls. The measurements based on the lidar point cloud data are accurate with an error of 2 mm at 10 meters, enabling high resolute and accurate assessments. As for the accelerometers, one setup with sixty minutes of ambient vibrations data collection was performed. Twenty unidirectional accelerometers were installed on the basement, ground, second, fourth, eighth, tenth and roof floors at southwest and northeast corners to capture the torsional and translational acceleration structural response. The collected data can be used to perform system identification throughout operational modal analysis to demonstrate the dynamic and modal properties of the structures. Both of the lidar and system identification sensing techniques provide essential input to establish and calibrate a detailed finite element model. The outputs are used to validate through the comparison of modal frequencies obtained in operational modal analysis method. Besides, the finite element model also provides a detailed response and insight to understand performance under future earthquakes.

Keywords: Lidar, Deformation quantification, System identification, 2017 Central Mexico Earthquake

INTRODUCTION

The 2017 Central Mexico (Puebla) earthquake occurred at 13:14 local time on September 19, 2017, with a moment magnitude of 7.1. The focal depth is approximately 50 km and the resulting ground shaking could be felt over the Mexico City area. Numerous aftershocks in the following days occurred with magnitudes in excess of 4.5. At least 40 structures collapsed during the earthquake and its aftershock sequence [1]. One representative damaged structure was a residential condo building located in the Hipódromo neighborhood. Prior to data collection by the authors, the structure was retrofitted for some exterior cracking and damage. On January 30, 2018, the authors visited the site to characterize the damage by collecting ambient vibration data and laser scanning using ground-based light detection and ranging (lidar). In this study, the combination of the collected data through these two platforms allow to characterize the dynamic properties and quantify the structures residual deformation after the earthquake sequence. Ambient vibrations collected by accelerometers at various levels of the structure were used to estimate the structure's vibration behaviors via operational modal analysis [2]. Lidar provides accurate geometry of the structure, which used to quantify and estimate drift of the structure after the event [3].

FIELD DETAILS

The sixteen-story residence building as showing in Figure 1a is a concrete structure with moment frames in the direction perpendicular to the roadway, and RC shear walls in the parallel direction to the roadway. The height of the structure is

approximately 42 meters, where typically two to four condos are located on each floor. As showing in Figure 1b, the structure had a footprint of 18 meters by 19 meters. Two elevators and a staircase are embedded at the center of each floor, from the basement to the top floor, which induces some potential torsional response in the structure. Exterior cracking was described by the building owner prior to the repair, while interior masonry severe damage was also witnessed by the research team. The basement columns were examined to have minor cracks, as well as on the ground floor.

(a) (b)

Figure 1. (a) Sixteen-story residence building (courtesy of Google Map) and (b) floor plan drawing.

DATA COLLECTION

Ambient vibration data collection

On January 30, 2018, the authors and research team members collected ambient vibration recordings. During afternoon and evening hours, 20 accelerometers, operating at 2048 Hz, were installed on seven different floor levels for approximately 60 minutes. Pedestrian traffic and moderate wind velocities primarily cause the excitation for ambient vibrations. As for the setup, four accelerometers were placed on the northwest and southeast corners at 2nd, 10th and top floors, two accelerometers installed on the southeast corner of the basement, ground, 4th, and 8th floors. The structure is not absolutely aligned along the cardinal north direction. Therefore, the accelerometer instruments were installed in the directions parallel (northeast) and perpendicular (southeast) to the structure. Due to the existing residence occupation during the visit, the authors were not permitted to enter all floors and access the corners.

Lidar point cloud data collection

Ground-based lidar has been used in structural engineering for various applications. Such applications include measurements, damage characterization, and deformation quantification due to lidar point clouds high level of accuracy [4]. The output format is three-dimensional point cloud data, which can be permanently preserved. The accuracy can reach a sub-centimeter level for small sites or structures [5]. However, the accuracy varies, which is a function of lidar settings, scan distance, and surface reflectivity. During the site visit and due to equipment availability, the lidar scan dataset was collected in the evening of February 1, 2018. Thirteen scans were collected by a Faro Focus3D s150 lidar scanner from all sides of the structure considering the accessibility in the built-up urban environment. For the lidar scanner settings, the vertical angular area is 90° to -60°, horizontal angular area ranged from 50° to 180° due to the coverage, occlusion, and selected scan locations. The resolution and quality settings were set as 1/4 and 4x. Since the data was collected in the late evening, no color information (RGB indices) was collected. The scan locations are shown in Figure 2a. For the scan registration procedures, 4-6 correspondences between each two closest scans were needed to be manually picked as an alignment reference. Objects such as points, slabs, spheres, planes, etc. can be identified as targets for referencing the corresponding scans. After forcing the correspondences between scans, target-based and cloud-to-cloud alignments were applied to tighten the registration. As a result, the registered point cloud is displayed in Figure 2b, the overall mean registration error was at a sub-centimeter level of 6.5 mm.

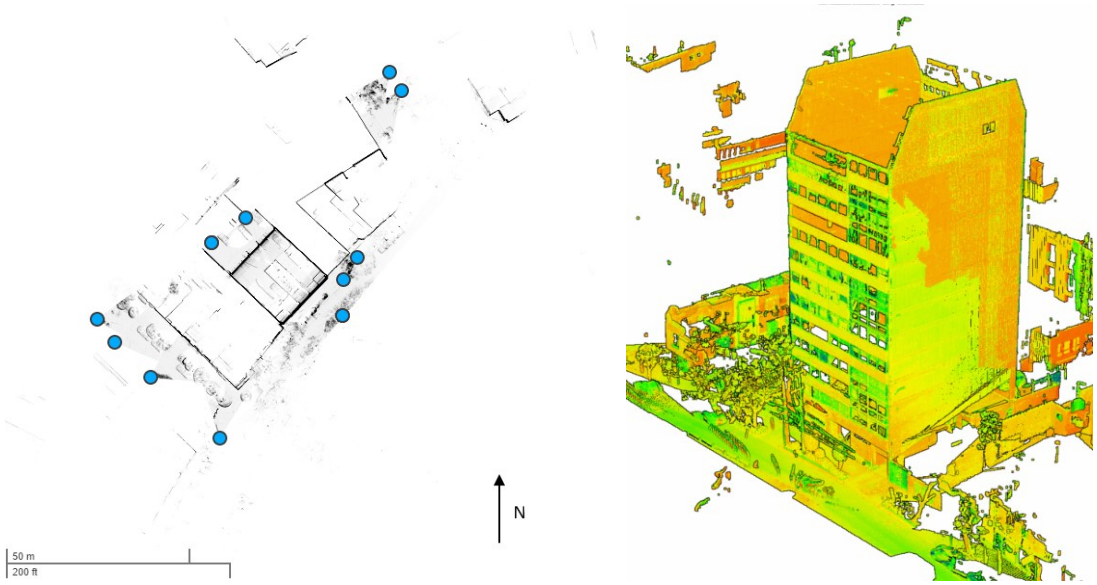

(a) (b)

Figure 2. (a) Lidar scan locations, (b) Isometric view of registered point cloud colorized by intensity.

STRUCTURAL ASSESSMENT

Previous Work

One of the more popular nondetective techniques for structural health monitoring is the use of ambient vibrations to conduct a system identification, an estimation of the modal properties [6][7]. While this is popular, it does not provide a full diagnosis of the structure. The ability to collect various data typologies including point clouds and vibrations has shown to be an effective technique for objective damage detection [8]. Specifically from the point clouds, the structural residual drift and surface defects can be quantified and related to the estimated modal properties [12]. One example of this application is in Wood et al. [7]. In this study, the authors performed system identification and a quantified damage assessment on a five-tiered pagoda style temple in Nepal post-2015 Gorkha Earthquake using ambient vibrations, lidar, and a model-updated finite element model. In this study, the authors computed the first three excited modes and noted a nearly 16.8% period elongation in the fundamental mode, in comparison to pre-earthquake data. Complementary to the vibration, lidar point clouds were also collected for accurate dimensions measurement due to the lack of structural plans, as well as damage characterization. The point cloud was analyzed for global deformation via torsional drift estimates and local deformation via quantification of the spalling and cracks in the first floor using a pattern recognition algorithm.

Identification of natural frequencies

Specific to this study, the entire 60 minutes of recording were used for the preliminary assessment to estimate the natural frequencies and operational deflected shapes. Initially, the data was filtered and subdivided to minimize the uncertainties via spectral averaging. For each channel, the acceleration time histories was first downsampled to 256 Hz and filtered in the frequency range of 0.2 Hz to 4 Hz, matching the range of interest for this structure. The overall structural modal natural frequencies were identified initially by peak picking method. The natural frequencies were able estimated as 0.458 Hz, 0.773 Hz, 1.079 Hz, 1.673 Hz, 2.983 Hz, and 3.416 Hz. Out of all of these modes, only mode three demonstrates a torsional response while the other five modes are translational-dominated in nature.

Due to the complexity of loading conditions, ARTeMIS software is used to perform the system identification process. ARTeMIS software is a commonly utilized software for system identification processing [13], which incorporates the stochastic subspace identification (SSI) method. The first six modes are identified and shown in the stability diagram in Figure 3. Table 1 and Figure 4 summarize the identification process, including the operational deflected shapes which are commonly akin to mode shapes. Note while the values are damping are reported in Table 1, these values may not represent the observed of damping present during the moderate level accelerations. Comparing the deflected shapes in Figure 4, it can be summarized that mode three and mode four have higher amounts of energy in the stabilization diagram.

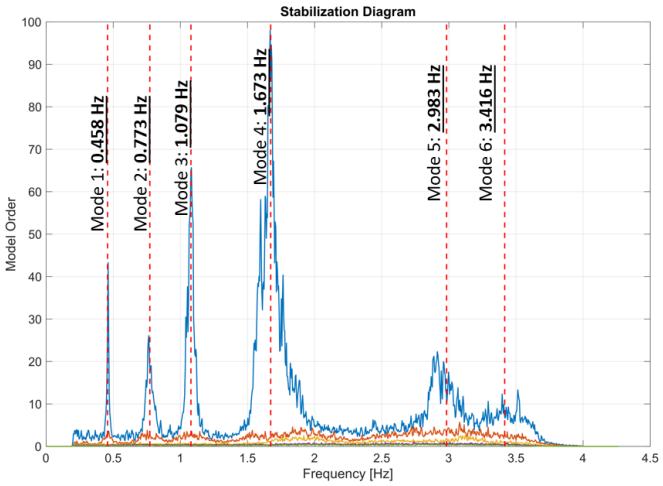

Figure 3. Modal natural frequencies estimation.

Table 1. ARTeMIS identified modes.

Mode	Frequency (Hz)	Damping (%)	Complexity (%)	Motion
Mode 1	0.458	2.218	1.001	Translation parallel to roadway
Mode 2	0.773	2.389	1.648	Translation perpendicular to roadway
Mode 3	1.079	1.968	1.320	Torsional
Mode 4	1.673	3.075	1.184	Translation parallel to roadway
Mode 5	2.983	2.888	2.250	Translation parallel to roadway
Mode 6	3.416	1.529	1.529	Translation perpendicular to roadway

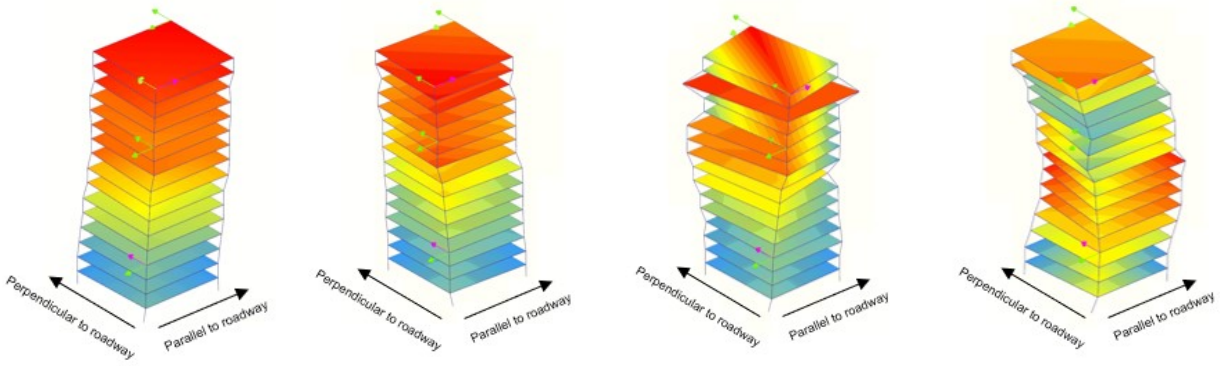

(a) (b) (c) (d)

Figure 4. Operational deflected shapes from ARTeMIS: (a) mode one, (b) mode two, (c) mode three, and (d) mode four.

Lidar point cloud assessment

The lidar point cloud data was used to assess the residual deformation and quantify deformation profiles. To accomplish this task, initially, the depth maps for two side walls (perpendicular to the roadway) were developed, which were exterior RC shear walls. With the assumption that the vertical direction of the point cloud data is aligned with the direction of gravity. In this study, the lidar scanner has a vertical alignment accuracy of 19 arcseconds, which equates to a 3 mm measurement error at the full height of the structure at 42 meters. Measuring from the ground floor as 1st floor instead of the basement to the roof, the nomenclature and a depth map for each wall is created as shown in Figure 5. The depth map colorizes point cloud into 1 cm color bins according to the local deformation in the out-of-plane direction, which gives an overview of the salient residual deformation features. The depth maps results suggested that the structure is leaning in the northeast direction as elevation increases. This is up to a maximum value of 38 cm.

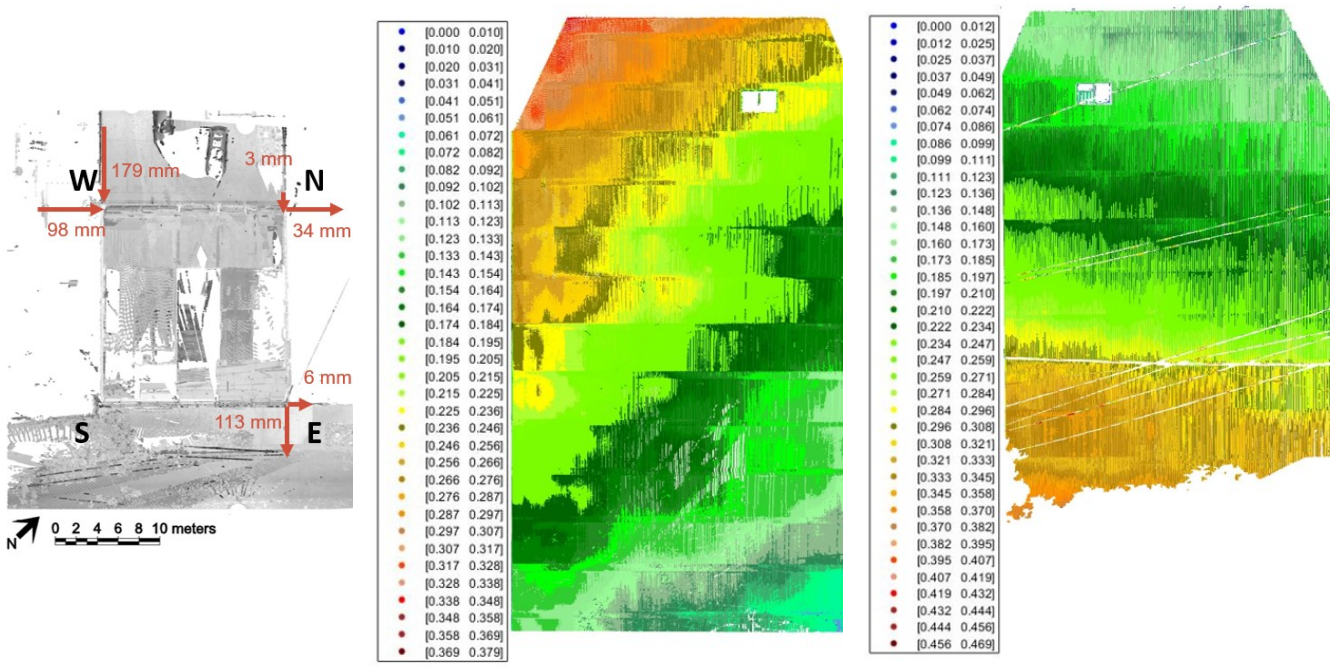

(a) (b) (c)

Figure 5. (a) Structure's top view and the nomenclatures with roof deformation values, (b) northeast wall depth-map in the out-of-plane direction, and (c) southwest wall depth map in the out-of-plane direction (white spaces near the roof are due to occlusion of windows).

The deformation profiles of each building corner were created to further investigate the residual deformation. The deformation profile analysis was only carried out for three corners of the structure due to significant occlusion at the southwest corner. Significant tree cover occluded this area of the structure at the time of data collection. The residual deformation for each corner is measured for the three corners, as demonstrated in Figure 6 and summarized in Table 2. The deformation profiles of the west and east corners in the northwest direction suggested these two corners are leaning in the southeast direction. Deformation profiles of the north corner (in both directions) had values of 98 mm and 179 mm and the east corner deformation profile in the northeast direction of 6 mm demonstrate that the structure has relatively smaller deformations in comparison to the west corner. In addition, the upper level of structure is leaning towards northeast and southeast directions, which corresponds to depth maps findings. These deformations can be correlated to system identification results that third and fourth mode were potentially dominate, which is torsional and translational response along the northeast direction. In addition, the residual deformation is due to torsional dynamic behavior.

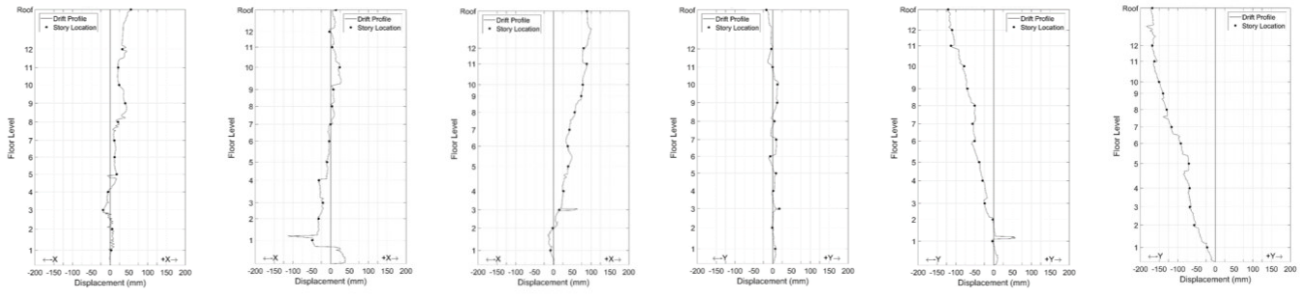

(a) *(b)* *(c)* *(d)* *(e)* *(f)*

Figure 6. Deformation profiles: (a)north corner on northeast direction, (b) east corner on northeast direction, (c) west corner on northeast direction, (d) north corner on northwest direction, (e) east corner on northwest direction, and (f) west corner on northwest direction.

Table 2. Comparison of corner deformations.

Story	Northeast (mm)			Northwest (mm)		
Level	N	E	W	N	E	W
1	2	-7	-48	6	-22	-3
2	5	-2	-31	-1	-56	-2
3	-18	15	-20	17	-68	-23
4	-5	26	-31	1	-68	-29
5	17	38	-9	8	-70	-38
6	11	38	-4	-6	-92	-50
7	11	42	0	9	-116	-56
8	20	56	3	4	-130	-50
9	40	73	6	11	-139	-69
10	24	77	23	12	-150	-78
11	21	88	3	0	-162	-113
12	32	80	-3	-3	-168	-110
Roof	34	98	6	-3	-179	-113

CONCLUSIONS

This study focuses on the preliminary damage assessment of a sixteen-story reinforced concrete residence building following the 2017 Central Mexico earthquake and its aftershock sequence. The assessment process was conducted through collecting and analyzing point cloud and ambient vibration data to study the structure post-earthquake health state. A system identification process using ambient vibrational data provided the dynamic and modal properties of the structure, while the lidar point cloud was used to assess the structure's residual deformation and tilt. Investigating the results from system identification and lidar point cloud assessment, mode three (torsional) and mode four (translation parallel to the roadway) can be potentially categorized as governing modes. Residual deformations are estimated to be from 3 mm to 179 mm at the roof level at its corners indicating that the structure is leaning towards the northeast. This building is located in the Mexico City seismic zone IIIA, which was classified as a soft soil due to the lake basin[14]. Natural frequencies of mode three and mode four are 1.079 Hz and 1.673 Hz, which are near the dominate basin period of 1.25 Hz in zone III [15]. This geotechnical condition and the observed damage pattern are in general agreement. Future work will be built on these findings, including the construction of a model-updated finite element model to validate these findings as well as investigate the seismic vulnerability.

ACKNOWLEDGMENTS

Travel funding was primarily provided for the University of Nebraska, Lincoln (UNL) team by the Department of Civil Engineering and the College of Engineering. Supplemental travel support was provided by National Science Foundation (NSF), under award number 1811084. The authors would like to graciously acknowledge the team members for assisting the field data collection at this structure including Prof. Andreas Stavridis and Mr. Supratik Bose from University at Buffalo, Ms. Lauren Benstead from California Polytechnic State University, and Mr. William (Willy) Rosenblatt from Wiss, Janney, Elstner Associates, Inc. Additional field support was provided by Prof. Santiago Pujol, Prof. Ayhan Irfanoglu, and Mr. Prateek Shah of Purdue University and Prof. Gilberto Mosqueda and Mr. Patrick Hughes from the University of California, San Diego. The authors also would also like to express their thanks for the support of FARO Technologies for the last minute equipment loaner, particularly Mr. Alex Shiah, Mr. Leobardo Nunez, and Mr. Jacob Eveland. This paper does not constitute a standard, specification, or regulation.

REFERENCES

[1] Semple K., Villegas P., and Malkin E., (2017). "Mexico Earthquake Kills Hundreds, Trapping Many Under Rubble." The New York Times. https://www.nytimes.com/2017/09/19/world/americas/mexico-earthquake.html

[2] Yousefianmoghadam S., Song M., Stavridis A., Moaveni. B. (2015) "System Identification of a Two-11 Story Infilled RC Building in Different Damage States." *Proceedings of Improving the Seismic Performance of Existing Buildings and Other Structures*, San Francisco, CA, 2015 607-618.

[3] Wood R. L., and Mohammadi M. E. (2015). "LiDAR scanning with supplementary UAV captured images for structural inspection." *International LiDAR Mapping Forum*, Denver, CO, USA.

[4] Bose, S., Nozari, A., Mohammadi, M.E., Stavridis, A., Babak, M., Wood, R., Gillins, D. and Barbosa, A., (2016). "Structural assessment of a school building in Sankhu, Nepal damaged due to torsional response during the 2015 Gorkha

earthquake." *Proceedings 34th IMAC, A Conference and Exposition on Structural Dynamics,* SEM, Orlando, FL USA, Springer, Volume 2, 31-41.

[5] Faro. (2016). *Faro laser scanner Focus 3D: features, benefits & technical specifications*. FARO Technologies, Lake Mary, FL, USA. http://www.gb-geodezie.cz/wp-content/uploads/2016/01/FARO_-Focus_3D.pdf

[6] Doebling S.W., Farrar C. R., Prime M. B., and Shevitz D.W., (1996). *Damage identification and health monitoring of structural and mechanical systems from changes in their vibration characteristics: a literature review*. No. LA--13070-MS, Los Alamos National Lab, NM, USA.

[7] Wood R. L., Mohammadi M. E., Barbosa A. R., Kawan C. K., Shakya M., and Olsen M. J. (2017). "Structural damage assessment of five tiered pagoda style temple." *Earthquake Spectra*. 1(33), 10.1193/121516EQS235M.

[8] Wood R. L., (2014). "Methods of structural damage characterization for infrastructure." *34th Annual Structural Congress, Structural Engineering Association of Nebraska,* Omaha, NE, USA, 12pp.

[9] Olsen M. J., Cheung K. F., YamazakI Y., Butcher S., Garlock M., Yim S., McGarity S., Robertson I., Burgos L., Young Y. L. (2012) "Damage assessment of the 2010 Chile earthquake and tsunami using terrestrial laser scanning." *Earthquake Spectra*. 28 (1), 179-197, 10.1193/1.4000021.

[10] Olsen M.J., Kuester F., Chang B.J., and Hutchinson T.C. (2010). "Terrestrial Laser Scanning-Based Structural Damage Assessment." *J. Comput. Civ. Eng.,* 2010.24:264-272, 10.1061/(ASCE)CP.1943-5487.0000028.

[11] Barbosa A.R., Fahnestock L.A., Fick D.R., Gautam D., Soti R., Wood R., Moaveni B., Stavridis A., Olsen M.J. and Rodrigues H. (2017). "Performance of medium-to-high rise reinforced concrete frame buildings with masonry infill in the 2015 Gorkha, Nepal, Earthquake." *Earthquake Spectra*, 33(S1), 197-218.

[12] Yu H., Mohammed M.A., Mohammadi M.E., Moaveni B., Barbosa A.R., Stavridis A. and Wood R.L. (2017). "Structural identification of an 18-story RC building in Nepal using post-earthquake ambient vibration and lidar data." *Frontiers in Built Environment* 3, 10.338 9/fbuil.201700011.

[13] Calrec Audio Ltd. (2017). *ARTEMIS installation & technical manual.* England, UK. https://calrec.com/wp-content/themes/calrec/pdf/Artemis%20Installation%20Manual%20(926-149%20Iss27%20Lo).pdf

[14] NTCS-04. (2004). Normas Técnicas Complementarias para diseño por sismo. Gaceta oficial del Distrito Federal, México.

[15] Chávez-García F.J., Cuenca J., Lermo J. and Mijares H. (1995). Seismic microzonation of the city of Puebla, Mexico.